Biomarker Signature Discovery from Mass Spectrometry Data

Ao Kong, Chinmaya Gupta, Mauro Ferrari, Marco Agostini, Chiara Bedin, Ali Bouamrani, Ennio Tasciotti, and Robert Azencott

Abstract—Mass spectrometry based high throughput proteomics are used for protein analysis and clinical diagnosis. Many machine learning methods have been used to construct classifiers based on mass spectrometry data, for discrimination between cancer stages. However, the classifiers generated by machine learning such as SVM techniques typically lack biological interpretability. We present an innovative technique for automated discovery of signatures optimized to characterize various cancer stages. We validate our signature discovery algorithm on one new colorectal cancer MALDI-TOF data set, and two well-known ovarian cancer SELDI-TOF data sets. In all of these cases, our signature based classifiers performed either better or at least as well as four benchmark machine learning algorithms including SVM and KNN. Moreover, our optimized signatures automatically select smaller sets of key biomarkers than the black-boxes generated by machine learning, and are much easier to interpret.

Index Terms—MALDI/SELDI data, ovarian cancer, colorectal cancer, biomarker selection, automatic signature discovery

1 Introduction

EARLY detection and risk assessment of cancer are crucial for successful intervention strategies. Identification of validated biomarkers, as a non-invasive screening method, is recognized as a major breakthrough in cancer detection [1]. Human body fluids such as serum or plasma are easily accessible sources of biomarker discovery, due to their wide range of molecular components linked to cellular metabolism by-products. In proteome analysis, proteins with low molecular weight (LMW) are of great interest, because cellular and extracellular enzymatic events generate small fragments, playing an important role at the level of cancer-tissue micro-environment [2]. Mass spectrometry techniques are considered to be a promising approach for LMW biomarker discovery.

Laser desorption ionization, either surface-enhanced (SELDI) or matrix-assisted (MALDI), are the two commonly used techniques to generate mass spectrometry data set. Each such mass spectrum provides thousands of mass-to-charge (m/z) ratios paired with corresponding peptide intensities. Experimental design for biomarker discovery requires adequate statistical sampling, appropriate handling and storage of serum or plasma samples until analysis, mass spectrometry processing of the samples, and detailed data analysis of the generated mass spectra. Our paper focuses only on this last step.

To handle the high dimensionality and inherent variability of biomedical mass spectra, "machine learning" algorithms have been applied to automatic discriminate between mass spectra. Unsupervised learning, such as clustering [3] or self-organizing maps [4], has been used to partition mass spectrometry data sets into homogeneous subgroups. Supervised learning, which analyzes pre-classified mass spectrometry data sets to generate automated classifiers, has been applied for cancer discrimination: artificial neural networks [5], K-nearest neighbors (KNN) [6], decision trees (DT) [7], [8], [9], [10], random forests (RF) [11], linear and quadratic discriminant analysis [12], support vector machines (SVM) [13], [14], [15]. Machine learning techniques have often yielded good classification accuracy, but they typically generate "black-box" classifiers, which are not easily interpreted biologically. To develop more pragmatic mass spectrometry classifiers, a key step is to automatically discover "signatures", i.e., combinations of a small number of protein biomarkers strongly discriminating between cancer states [16], [15], [17], [18].

We have developed new algorithms for automatic discovery of biologically interpretable signatures discriminating between various cancer states, by automated analysis of mass spectrometry data sets acquired from multi-stages cancer patients groups. We applied simulated annealing optimization techniques [19], [20], [21] to maximize discriminating power among all possible signatures.

We have tested our signature discovery algorithm on a new MALDI-TOF data set for colorectal cancer and two well-known ovarian cancer SELDI-TOF data sets. We have generated explicit signatures with high discriminating power between the various cancer patients groups involved in these data sets. We have compared performances between our optimized signature based classifiers and several benchmark machine learning techniques.

2 Data Sets

2.1 Colorectal MALDI-TOF Data Set

One hundred and four colorectal cancer samples and 15 control samples were provided by first Surgical Clinic, Department of Surgical, Oncological and Gastroenterological Sciences, University of Padova, Italy. Between 2002 and 2005, the 104 cancer patients underwent surgeries and histopathological diagnosis. Among them, 27 were diagnosed with colorectal pre-cancer lesion (Adenoma), 40 with Early Colorectal cancer (stage I or II), and 37 with Late Colorectal cancer (stage III or IV). The 15 healthy patients all received colonoscopy and were diagnosed to be unaffected.

A 10 ml blood sample was collected from each patient into a DB Vacutainer during the surgery or colonoscopy and transferred to the laboratory within 4 hours of collection, to be centrifuged at 3,000 rpm for 10 min. Plasma samples were then collected from the supernatant and stored in aliquots at -80° C in the Tumor Tissue Biobank of Surgical Clinic I as well as during transportation, until analysis.

For efficient removal of high molecular weight proteins and for specific isolation and enrichment of LMW species present in 15μl of plasma, we used a novel three steps size-exclusion strategy based on Mesoporous silica chips, fabricated by Dept of Nanomedicine (Methodist Hospital Research Institute, Houston, Texas) [22]. Mass spectra were acquired in linear positive-ion mode (range 800-10,000 "m/z" ratio) on a Voyager-DE-STR MALDI TOF Mass Spectrometer (Applied Biosystems, Framingham, MA) at Research Center of Protein Chemistry Core Laboratory (University of Texas Health, Houston, Texas). The manufacturer provided spectrometer accuracy was 0.3 percent. Only one blood plasma sample was extracted from each subject, but two "replicate" mass spectra were acquired from each blood plasma sample.

In total, 238 mass spectrometry replicates were acquired from four patients groups, with two mass spectrometry replicates per patient: the Control group CTR of 15 patients, the Adenoma group ADE of 27 patients with precancer lesions, the group ECR of 40

Q1

- *A. Kong and C. Gupta are with the Department of Mathematics, University of Houston, TX.*
- *M. Ferrari and E. Tasciotti are with the Department of Nanomedicine, The Methodist Hospital Research Institute, Houston, TX.*
- *M. Agostini is with the Department of Surgery, Oncology and Gastroenterology, 1st Surgical Clinic, University of Padova, Italy, and the Department of Nanomedicine, The Methodist Hospital Research Institute, Houston, TX.*
- *C. Bedin is with the Nano Inspired Biomedicine, Istituto di Ricerca Pediatrica (IRP) - Fondazione Città della Speranza, Padova, Italy, and the Department of Surgery, Oncology and Gastroenterology, 1st Surgical Clinic, University of Padova, Italy.*
- *A. Bouamrani is with the Clinatec, CEA-LETI, Grenoble, France.*
- *R. Azencott is with the Department of Mathematics, University of Houston, Houston, TX, and C.M.L.A. Ecole Normale Superieure, Cachan, France.*

Manuscript received 23 Oct. 2013; revised 19 Feb. 2014; accepted 28 Mar. 2014; date of publication xx xx xxxx; date of current version xx xx xxxx.
For information on obtaining reprints of this article, please send e-mail to: reprints@ieee.org, and reference the Digital Object Identifier below.
Digital Object Identifier no. 10.1109/TCBB.2014.2318718

patients with Early ColoRectal cancer (stage I-II), the group LCR of 37 patients with Late ColoRectal cancer (stage III-IV). We also studied the whole cancerous group CRC of 104 patients pooling together all three cancer groups ADE, ECR, LCR. Each mass spectrum provides about 36,900 m/z values between 800-10,000 on the x-axis and the associated "peptide intensities" on the y-axis.

2.2 Ovarian SELDI-TOF Data Sets

We have also tested our approach on two well-known mass spectrometry data sets of ovarian cancer, which can be freely downloaded from NCI-FDA clinical proteomics databank (http://home.ccr.cancer.gov/ncifdaproteomics/ppatterns.asp).

The data set "4-3-02" consists of 116 control (normal or benign patients) mass spectra and 100 ovarian cancer mass spectra, acquired manually, using a WCX2 protein chip and a Ciphergen PBS1 SELDI-TOF mass spectrometer with 0.1 percent accuracy. Each mass spectrum listed 15,154 m/z values in the 0-20,000 range. Baselines were removed prior to public access. This data set was studied by [4], [6], [23] who respectively reported discrimination accuracies of 97.5, 100 and 86.66 percent.

The data set "8-7-02" gathers 91 control and 162 ovarian cancer mass spectra, acquired by robotic hardware using a WCX2 chip but with an upgraded PBSII SELDI-TOF mass spectrometer with 0.1 percent accuracy. Each spectrum gave 15,154 m/z values in the 0-20,000 range. This data set was studied by [6], [24], [25] and [23], with reported discrimination accuracies of 100 percent.

3 Methods

3.1 Pre-Processing

To lower data dimensionality and reduce acquisition "noise", pre-processing of mass spectra is a standard first step, often implemented via commercial interactive softwares. Pre-processing principles are well known, but implementation details vary considerably, and are often not accessible in commercial softwares. For better context control, we have developed our own sequence of pipelined pre-processing steps for each raw mass spectrum.

1) Intensities are rescaled (normalized) so that total peak intensity equals 1.
2) Smoothing at current abscissa x is then implemented by moving average on a sliding window $x \pm ux$, where the fixed ratio u is user-defined.
3) Noise values are extracted by subtracting smoothed spectrum from raw spectrum. Local noise level at x is evaluated on a sliding window $x \pm vx$ where the ratio v is user-defined.
4) Baseline is computed by moving medians within sliding windows $x \pm wx$ where ratio w is user-defined. Baseline is then removed from smoothed spectrum. Using medians instead of means avoids discarding small peaks in the vicinity of large peaks.
5) Peaks above baseline are then extracted from the smoothed spectrum to retain only the "strong peaks", for which "peak strength" (ratio of peak height to local noise level) is higher than a threshold th fixed by the user.

3.2 Reference Biomarkers and Activation Frequencies

For a MALDI or SELDI spectrometer with manufacturer accuracy ρ, any peptide with "true" m/z ratio x will yield randomly shifted acquisition values within the "uncertainty window" $x \pm \rho x$. In view of these acquisition uncertainties, we fix a sequence of "reference biomarkers" B_j at abscissas $B_j = a(1+\rho)^j$, with $0 \leq j \leq n$ where $B_0 = a$ and $B_n = b$ are the smallest and largest observed m/z values among all spectra in our training data set.

We say that a reference biomarker B is "activated" by a mass spectrum M if at least one strong peak detected in M is positioned within the uncertainty window of B. Otherwise, we say that "B is not activated by M".

Given two distinct groups G^+ and G^- of observed mass spectra, we characterize each reference biomarker B by its "activation frequencies" $f^+(B)$ and $f^-(B)$, defined as percentages of mass spectra which respectively activate B within G^+ and within G^-.

3.3 Selection of Biomarkers with High Discriminating Power

One can prove that the most powerful test to discriminate between G^+ and G^- on the basis of the presence or absence of a single biomarker B is achieved by adequate thresholding for the ratio of activation frequencies $f^+(B)/f^-(B)$. This suggests quantifying the G^+ detecting power of a biomarker B by $D^+(B) = f^+(B)/f^-(B)$ and its G^- detecting power by the inverse ratio $D^-(B) = f^-(B)/f^+(B)$. We say that B is a G^+ biomarker if $D^+(B) > 1$ and a G^- biomarker if $D^-(B) > 1$.

To seek optimal signatures combining small numbers of biomarkers, we first select a tentative target pool $TP(2k)$ of $2k$ highly discriminating biomarkers, namely the k biomarkers with highest $D^+(B)$ and the k biomarkers with highest $D^-(B)$.

Good generalization capacity requires k to be small while high discriminating power forces k to be large. So we successively implement our signature discovery algorithm for increasing values of k, and later select an optimal k.

3.4 Automatic Signature Discovery

Given a training data set involving two pre-classified groups of mass spectra G^+ and G^-, we seek to generate various automated classifiers of arbitrary mass spectra M and compare their performances. We systematically evaluate the performance level of any classifier by $PERF = (p^+ + p^-)/2$ where p^+ and p^- are the frequencies of correct classification for the spectra belonging respectively to G^+ and to G^-.

A signature Sig will be any fixed list of r biomarkers picked within the target pool $TP(2k)$ just defined. Given any spectrum M, we count, within the signature Sig, the number $u(M)$ of G^+ biomarkers activated by M and the number $v(M)$ of G^- biomarkers which are NOT activated by M. The "G^+ score" of M for the signature Sig is then defined by $s^+(M, Sig) = (u(M) + v(M))/r$. Clearly, M will achieve a high G^+ score if most of the G^+ biomarkers belonging to signature Sig are actually present in M, and if simultaneously most of the G^- biomarkers belonging to Sig are absent in M. The signature Sig will have high G^+ detecting power if $s^+(M, Sig)$ is high for M in G^+ and low for M in G^-.

Exchanging the roles of G^+ and G^- symetrically defines the "G^- score" $s^-(M, Sig)$ of M for the signature Sig. Then Sig will have high G^- detecting power if $s^-(M, Sig)$ is high for M in G^- and low for M in G^+.

When one fixes a scoring threshold $0 < c < 1$, the signature Sig determines a $G+$ classifier by assigning any observed spectrum M to G^+ if $s^+(M, Sig) \geq c$ and to G^- otherwise. The performance level $PERF(c, Sig)$ of this classifier is defined as above by its average frequency of correct classification $(p^+ + p^-)/2$. For each Sig, there is an easily computable optimal threshold $c = c^*$ maximizing $PERF(c, Sig)$ over all potential thresholds c. This maximized performance $J^+(Sig) = PERF(c^*, Sig)$ will define the "G^+ detecting power" of signature Sig.

Exchanging G^+ and G^-, as well as the scores $s^+(M, Sig)$ and $s^-(M, Sig)$ we similarly define the G^- detecting power $J^-(Sig)$ of signature Sig.

Among all potential signatures Sig within our biomarkers target pool $TP(2k)$, we will now seek two optimized signatures, Sig^+ maximizing the G^+ detecting power $J^+(Sig)$ and Sig^- maximizing the G^- detecting powers $J^-(Sig)$. But $J^+(Sig)$ and $J^-(Sig)$ have many local maxima, and the set of all potential signatures within $TP(2k)$ has very large cardinal. To solve this combinatorial challenge, we implement the separate maximizations of $J^+(Sig)$ and of $J^-(Sig)$ by Simulated Annealing as described next.

3.5 Optimized Signature Discovery by Simulated Annealing

Simulated annealing is a powerful stochastic descent technique to search for the global maximum of an "objective function" defined for configurations belonging to a very large discrete space [19], [20], [21]. Here, we implement a simulated annealing search to find an optimal signature Sig^+ maximizing the G^+ detecting power $J^+(Sig)$ over the set of all potential signatures Sig included in our target pool $TP(2k)$ of $2k$ biomarkers.

Each potential signature Sig can be naturally coded as a binary sequence of length $2k$, where the coordinates equal to 1 correspond exactly to the biomarkers which belong to the list Sig. Starting from any initial signature, we successively visit each one of its $2k$ binary coordinates, and randomly modify this coordinate according to a "simulated annealing rule". This procedure is repeated after each sequence of $2k$ steps.

At step n, the currently visited signature coordinate is randomly replaced by 0 or 1. This tentatively replaces the current signature Sig_n by a new signature Sig_{n+1}, which is accepted or rejected with a precise probability explicitly computed in terms of $J^+(Sig_{n+1}) - J^+(Sig_n)$ and of a virtual "temperature" $T_n = (0.95)^n$ [19]. This iterative search essentially stops when $T_n \equiv 0$.

Our numerical implementation involves $200 \times 2k$ updates of signature coordinates per simulated annealing search. We implement multiple simulated annealing searches and retain the signature Sig^+ achieving the highest value for the G^+ detecting power $J^+(Sig)$.

Similar simulated annealing searches are implemented to discover a signature Sig^- maximizing the G^- detecting power $J^-(Sig)$.

3.6 Signature Based Patient Classification

After computing two optimal signatures Sig^+ and Sig^-, each mass spectrum M can be characterized by its G^+ score $s^+(M) = s^+(M, Sig^+)$ and its G^- score $s^-(M) = s^-(M, Sig^-)$. We then classify any new spectrum M into G^+ if $s^+(M) \geq \alpha\, s^-(M) + \beta$, and into G^- otherwise. The best coefficients α, β are computed by maximizing the performance $(p^+ + p^-)/2$ of this signature based classifier over the training data set. Since Sig^+ and Sig^- were restricted to be within the biomarker target pool $TP(2k)$, we denote by $PERF(2k)$ the performance level of this optimized signature based classifier.

When we have two replicate spectra M_1, M_2 per patient, we replace $s^+(M_1)$ and $s^+(M_2)$ by their average s^+ and do the same for s^-, before constructing as above the best separator based on the sign of $s^+ - (\alpha\, s^- + \beta)$.

We progressively increase k starting with a small value, and repeat the whole signature discovery procedure until $PERF(2k)$ reaches a satisfactory plateau.

Representing each mass spectra M by the planar point $[s^+(M), s^-(M)]$ provides an efficient graphic display of G^+ and G^- (see example in Section 4.3).

3.7 Cross Validation of Classifier Performance

To evaluate as defined above the performance of any classifier we need to estimate the frequencies p^+ and p^- of correct decisions when the patient is resp. in G^+ or in G^-. Since our data sets have moderate size, we estimate p^+ and p^- by a classical 10-fold cross validation analysis. So we randomly split the whole data set into 10 subsets and at each cross validation round, nine of these subsets are used for training a classifier and the 10th subset becomes the testing set. The percentages p^+, p^- of correct decisions are computed within the left out 10th set. These training-testing steps are repeated 10 times, and we evaluate p^+, p^- by averaging the 10 partial estimates just obtained. To capture the variability of these p^+ and p^- estimates, this 10-fold cross validation is repeated for 100 such random partitions of the whole data set. This provides two samples of 100 estimates, one for p^+ and one for p^-. The mean and standard deviations of these two samples provide our final estimates of p^+ and p^-, as well as the associated 95 percent confidence intervals.

4 Results for Colorectal Cancer MALDI Data Set

Our colorectal cancer data set (see Section 2.1) involved 119 patients and 238 raw MALDI mass spectra (two replicates per patient): the control group CTR and the Colorectal Cancer group CRC, which was pre-classified according to cancer stage into three subgroups (Adenoma ADE, early cancer ECR, late cancer LCR). We have implemented our signature discovery algorithms for four discrimination tasks: CTR versus CRC, ADE versus ECR, ADE versus LCR, ECR versus LCR.

4.1 Pre-Processing Results

In our colorectal cancer data set, each raw spectrum listed roughly 37,000 distinct "m/z" ratios ranging from 800 to 10,000. Pre-processing was implemented as in Section 3.1, with pre-processing parameters set at $u = 0.0003, v = 0.017, w = 0.025, th = 2$. We thus detected an average of 330 strong peaks per spectrum. Fig. 1 displays the detected strong peaks for one typical raw mass spectrum within the m/z range [1,800, 2,000].

4.2 Biomarkers Target Pools

Our 842 reference biomarkers B_j were positioned at successive abscissas 800×1.003^j with $j = 0, 1, 2, \ldots$. For each benchmark discrimination task CTR vs CRC, ADE vs ECR, ADE vs LCR, ECR vs LCR, we then successively extracted target pools $TP(2k)$ of $2k$ highly discriminating biomarkers, with $2k = 2, 4, \ldots, 40$.

For each benchmark task and each k, we computed two optimized signatures Sig^+ and Sig^- within $TP(2k)$ and the performance level $PERF(2k)$ of the signature based classifier we have associated above to the pair of signatures Sig^+ and Sig^-.

Signature based discrimination between cancerous and control group (CRC versus CTR) reached perfect performance level 100 percent for $2k = 8$. For discrimination between cancer stages ADE versus ECR, ADE versus LCR, ECR versus LCR, our signature based classifiers reached their respective performance plateaus for $2k = 30, 40, 32$.

4.3 Detailed Results for Discrimination between Adenoma and Early Colorectal Cancer

For signature based discrimination between $G^+ = ADE$ and $G^- = ECR$, we display in Fig. 2 the iterative maximization of $J^+(Sig)$ by a simulated annealing search with a total of 6,000 temperature cooling steps. As above $J^+(Sig)$ is the G^+ detecting power, with $G^+ = ADE$. As Fig. 2 indicates, $J^+(Sig)$ reaches a maximum after roughly 4,100 simulated annealing steps and then stabilizes during the last 1,900 annealing steps. The optimal signature $Sig^+ = Sig^{ADE}$ achieves correct classification of single spectrum replicates with frequency $p^+ = 91\%$ within ADE and frequency $p^- = 95\%$ within ECR, yielding an ADE detecting power of 93 percent. The second optimized signature $Sig^- = Sig^{ECR}$ achieves an ECR detecting power of 95 percent.

Via the optimal signatures Sig^{ADE} and Sig^{ECR}, we compute for each patient an ADE score $s^{ADE} = s^+$ and an ECR score $s^{ECR} = s^-$. The 67 patients belonging to either ADE or ECR can then be viewed as planar points with coordinates $(x = s^{ADE}, y = s^{ECR})$, as

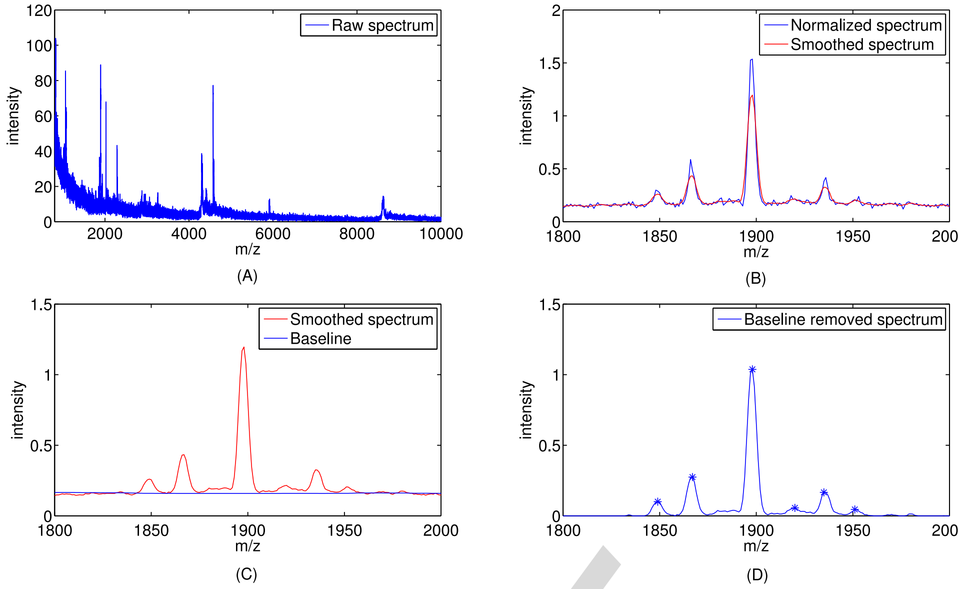

(A) (B) (C) (D)

Q2 Fig. 1. An example of raw spectrum with 36,930 distinct m/z values is presented in (A). Intermediate pre-processing results within the m/z range$[\,1{,}800, 2{,}000\,]$ are displayed in (B) and (C). (D) highlights the six peaks detected within this range.

displayed in Fig. 3 where final classification is then implemented by a linear separator.

4.4 Optimized Signatures for Colorectal Cancer Stage Discrimination

For each one of the colorectal cancer stage discrimination tasks ADE versus ECR, ADE versus LCR, ECR versus LCR, as well as for the much easier discrimination between cancerous and healthy patients CRC versus CTR, Table 1 exhibits separately the signature selected biomarkers discriminating in favor of each patient group. More precisely, for each discrimination task G^+ versus G^-, we pool together all the biomarkers belonging to at least one of the two optimized signatures Sig^+ and Sig^-; we then split this highly selective pool of biomarkers into two sets: the G^+ biomarkers and the G^- biomarkers, which we display separately. The simultaneous presence of several such G^+ biomarkers then strongly points to G^+ patients, with a similar interpretation for G^-.

With two replicates per patient on our colorectal cancer data set, the signature based classifiers just constructed for single replicates, are readily extended to pairs of replicates as outlined in Section 3.6. The performances p^+ and p^- of these "patient level" classifiers are summarized in the "patient level" panel of Table 2, where the "single spectrum level" panel reports the performance based on single replicate classification. These basic "single spectrum" performance levels for our signature based algorithms will be compared below to the single spectrum performances of machine learning algorithms in Section 4.5.

Discriminating the control group CTR from the union CRC of all three colorectal cancerous groups ADE, ECR, LCR, was the easiest of the four tasks studied here, and was achieved with 100 percent accuracy, by very short signatures. The three discrimination tasks between the three cancer stages ADE, ECR, LCR required longer signatures, to achieve fairly good classification levels.

4.5 Performance Comparisons with Machine Learning Techniques

Colorectal cancer detection by machine learning applied to MALDI/SELDI data has been studied by several publications. For discrimination between colorectal cancer and controls, [26] used support vector machine learning to achieve correct classification frequencies of $p^+ = 83 \pm 4\%$ and $p^- = 89 \pm 3\%$, [27] used decision trees to reach $p^+ = 65\%$ and $p^- = 90\%$, and [28] applied K-nearest

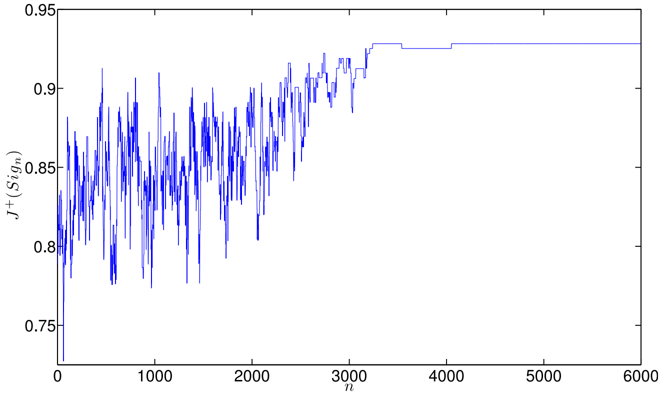

Fig. 2. Adenoma ADE versus Early Colorectal cancer ECR: simulated annealing search for an optimized signature Sig^{ADE} characterizing the Adenoma group. The ADE detecting power reaches its maximum 93 percent after roughly $4{,}100$ cooling steps and stabilizes at that level.

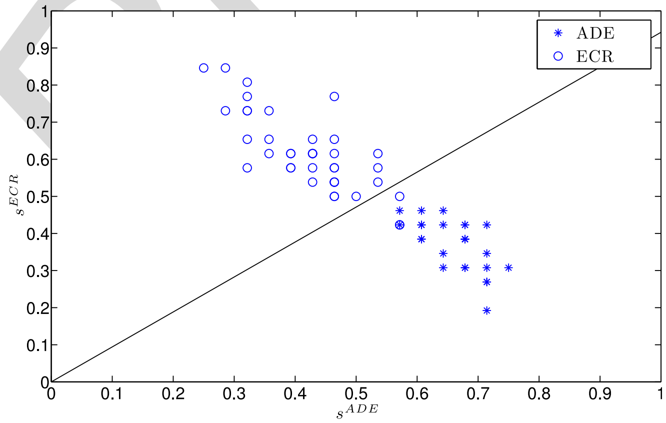

Fig. 3. Adenoma ADE versus Early Colorectal cancer ECR: planar display of patients scores (s^{ADE}, s^{ECR}), computed via the optimized signatures Sig^{ADE} and Sig^{ECR}. Signature based discrimination implemented as above classifies any patient in ADE whenever the scores of the patient's mass spectra verify $s^{ADE} > 1.06 s^{ECR}$.

TABLE 1
Biomarkers in Optimized Signatures for Colorectal Cancer Stage Discrimination

ADE vs ECR		ADE vs LCR		ECR vs LCR		CRC vs CTR	
1106	839	1146	819	921	819	1802	1202
1146	873	1192	839	1112	1029	3183	1439
1188	1261	1343	1246	1570	1032	3708	1652
1192	1288	1542	1261	1953	1210	4155	1657
1397	3610	1570	2651	2558	1213		
1579	3985	1845	2773	2589	2143		
1845	6283	2007	3844	4180	2331		
1851	7984	4180	7254	5033	2628		
2475	8630	4193	7587	6320	2807		
3675	8813	5186	7984	6339	3856		
5064		8032	8630	6894	4944		
6377			8813	6915	5829		
6416				7542	6226		
				8032	7889		
				8376			

For each discrimination task G^+ vs G^-, the biomarkers belonging to either Sig^+ or Sig^- are first pooled together, before splitting this pool into G^+ and G^- biomarkers, displayed in two distinct columns. In the signature based classification of a new mass spectrum M, the column under G^+ gathers the peak abscissas whose presence in M are strong indicators that M is of G^+ type. An analogous statement holds for G^-. For each one of these four discrimination tasks, the number of key biomarkers selected by each optimal pair of signatures remains quite moderate, namely 23, 23, 29, and 8.

neighbors to reach $p^+ = 66\%$ and $p^- = 46\%$. With 100 percent accuracy for colorectal cancer versus control, our signature discovery algorithm clearly outperforms these three previously published machine learning results.

We are not aware of previous publications on discrimination between colorectal cancer stages based on MALDI/SELDI data. Since our colorectal cancer MALDI data is not published, we have thus implemented four benchmark machine learning algorithms on each one of our colorectal cancer stages discrimination tasks: support vector machines with Gaussian kernel, K-nearest neighbor, decision tree and random forest.

As in [12], these machine learning methods classically characterize each biomarker through the t-statistic $t = \frac{|\mu^+ - \mu^-|}{\sqrt{(\sigma^+)^2 + (\sigma^-)^2}}$, where where μ^+, σ^+ and μ^-, σ^- are the means and standard deviations of the biomarker intensities observed in G^+ and G^-. The N biomarkers with the highest t-statistic are then selected as reference biomarkers. For $N = 2, 4, 6, 8, \ldots$, we have implemented these four benchmark machine learning techniques on all our colorectal cancer discrimination tasks. In each case, we then selected the N for which machine learning performance reached a first plateau. The implementation used the SVM, KNN, DT and RF toolboxes provided by MATLAB. Note that for SVM, we have carefully selected the best values for two key learning parameters (cost "tradeoff" and gaussian kernel "scale").

Performance comparisons between machine learning and our signature based discrimination are implemented for classification of single MALDI spectra, namely, at the "single spectrum level" of Table 2. Performances were evaluated by repeated 10-fold cross-validation as outlined in Section 3.7.

Among machine learning techniques, SVM is clearly superior to KNN, DT and RF. The number of biomarkers used by SVM is around 40 for the three delicate discriminations between cancer stages and 10 for the much easier cancer versus control task. Our signature based classifiers exhibit comparable performance levels with SVM for all the tasks, but offers two clear advantages over SVM: for comparable performances, our optimized signatures systematically involve less biomarkers than SVM, and the associated classifiers are fully and explicitly interpretable, which is not at all the case for the black box classifiers generated by SVM.

5 Results on Ovarian Cancer SELDI Data Sets

For all raw mass spectra in the published ovarian cancer SELDI data sets 4-3-02 and 8-7-02, pre-processing was implemented as

TABLE 2
Discrimination by Optimized Signatures: Performances on Colorectal Cancer Data

	ADE vs ECR		ADE vs LCR		ECR vs LCR		CRC vs CTR	
Single Spectrum level								
p^+ and p^-	88±5%	80±5%	85±5%	88±4%	83±5%	83±4%	100±0%	100±0%
Patient level								
p^+ and p^-	87±5%	87±5%	89±6%	89±7%	86±4%	86±4%	100±0%	100±0%

Discrimination between G^+ and G^- based on our optimized signatures is evaluated by the frequencies p^+ and p^- of correct classifications within G^+ and G^-. The p^+ and p^- estimates, and their 95 percent confidence intervals are obtained by repeating 100 times a 10-fold cross validation procedure. Performances on colorectal cancer data are given for single mass spectrum classification, as well as for two replicates classification (patient level).

TABLE 3
Performances on Colorectal Cancer Data: Comparison between Signature Based and Machine Learning Classifiers

	ADE vs ECR		ADE vs LCR		ECR vs LCR		CRC vs CTR	
Signatures	88±5%	80±3%	85±5%	88±4%	83±5%	83±4%	100±0%	100±0%
SVM	80±5%	91±3%	86±5%	91±3%	84±5%	85±4%	100±0%	100±0%
KNN	61±6%	74±4%	73±4%	84±4%	67±4%	78±4%	100±0%	100±0%
DT	56±10%	73±8%	78±6%	76±6%	70±8%	65±8%	99±1%	95±5%
RF	70±8%	88±4%	76±6%	88±3%	80±5%	77±5%	99±1%	98±2%

For discrimination between colorectal cancer mass spectra, we compare performances between signature based classifiers and four benchmark machine learning techniques SVM, KNN, DT, RF. For each discrimination task G^+ versus G^-, and for each type of classifier, we display side by side the frequencies p^+ and p^- of correct classification within G^+ and G^-. Q3

above, with windows size parameters set at $u = 0.0003$, $v = 0.017$, $w = 0.025$ and peak strength threshold $th = 2$. On data set 4-3-02, the baseline had been removed prior to publication. In both data sets, all publicly accessible mass spectra had been pre-aligned to a fixed list of 15,154 peak positions, which we also adopted as our list of reference biomarkers.

Our signature based classifiers were then implemented separately on the SELDI data sets 4-3-02 and 8-7-02 to discriminate between Ovarian Cancer patients and Control patients. Classification performance reached a plateau at biomarker target pool size $2k = 22$ for data set 4-3-02 and at target pool size $2k = 8$ for data set 8-7-02. Final performances were evaluated as above by repeated 10-fold cross validations.

For the SELDI data set 4-3-02, signature based classifiers achieved correct decision frequencies of 95±4% for the ovarian cancer group and 94±4% for the control group. These performances compare quite well with published results obtained on the same data set by other algorithms, namely $96.5 \pm 3.5\%$ and $93 \pm 6\%$ in [4], $96.5 \pm 3.5\%$ and $97.5 \pm 2.5\%$ in [6], 90 percent and 83.3 percent in [23]. For the SELDI data set 8-7-02, signature based classification reached 100 percent accuracy, which agrees with the results of previous studies [6], [24], [25], [23].

6 Conclusion

A natural goal for computer aided discrimination between various cancer stages or cancer types on the basis of proteomic "m/z" spectra acquired by MALDI or SELDI mass spectrometers is to select highly discriminating "signatures" gathering explicit small sets of biomarkers. This is a delicate task due to the well known repeatability and variability problems linked to proteomic mass spectra. Potential applications include software tools for early clinical diagnosis, as well as disease progression monitoring and evaluation of response to treatment.

A large number of machine learning studies have reportedly achieved good automated classification performances for specific data sets of proteomic mass spectra. Nevertheless, few machine learning algorithms have been incorporated into routinely and clinically usable software tools. This is in part due to the fact that machine learning generates "black box" classifiers with low biological interpretability.

In this paper we present and successfully test innovative algorithms to perform automated discovery of optimized short biomarkers signatures, to efficiently discriminate between given data sets of MALDI or SELDI mass spectra associated to various cancer stages. Our optimized signatures have the advantage of fairly direct biological interpretability.

Automated computer search for highly discriminating biomarkers signatures is an algorithmic problem with quite high computational complexity. This motivates our innovative use of simulated annealing optimization techniques to search for signatures with high discriminating power. We have combined this approach with efficient selection of target pools of potential biomarkers, and thus implemented powerful software tools for automated signature discovery.

We have first successfully tested our signature based mass spectrometry classifiers on a new experimental set of 238 MALDI-TOF mass spectra acquired from patients at various stages of colorectal cancer. Correct classification frequencies were good and compared quite favorably with the performance levels achieved on the same data set by four benchmark machine learning techniques: support vector machines, K-nearest neighbor, decision trees, random forest. Our signature discovery approach handles easy discrimination tasks (colorectal cancer versus control) certainly as well as all other machine learning techniques. For the more delicate discrimination between three colorectal cancer stages, the performances of our signature based classifiers were statistically indistinguishable from those of SVM, and these performance levels were clearly better than those for KNN, DT and RF. However, our optimized signatures had two key advantages over SVM: our signatures always required less biomarkers than SVM to achieve similar performances, and generated explicit and fully interpretable classifiers, instead of the black-box classifiers generated by SVM.

We have also tested our signature discovery techniques on two published data sets of SELDI-TOF mass spectra acquired from ovarian cancer patients. On these two ovarian cancer data sets, our signature based classifiers performed very well, and either matched or improved the performances achieved by other published techniques.

A key feature of our optimized signatures is that they do provide short lists of discriminating biomarkers identified by their "m/z" ratios. This is an important step to narrow down small sets of high priority biomarkers, to be targeted in further experimental studies or therapeutics research.

In future work, we intend to calibrate and test our signature discovery technique on MALDI and/or SELDI data sets acquired on breast cancer patients.

Acknowledgments

This study was supported in part by grants from the CARIPARO and AIRC Foundation. Biological samples were collected and stored by the Tumor Tissue Biobank of Surgical Clinic I. Data acquisition was partially funded by University of Texas Health Sciences.

References

[1] C. P. Paweletz et al., "Proteomic patterns of nipple aspirate fluids obtained by SELDI-TOF: Potential for new biomarkers to aid in the diagnosis of breast cancer," *Disease Markers*, vol. 17, pp. 301–307, 2001. Q4

[2] E. F. Petricoin and L. A. Liotta, "SELDI-TOF-based serum proteomic pattern diagnostics for early detection of cancer," *Current Opinion Biotechnol.*, vol. 15, pp. 24–30, 2004.

[3] T. C. W. Poon et al., “Comprehensive proteomic profiling identifies serum proteomic signatures for detection of hepatocellular carcinoma and its subtypes,” *Clinical Chemistry*, vol. 49, pp. 752–760, 2003.

[4] E. F. Petricoin et al., “Use of proteomic patterns in serum to identify ovarian cancer,” *Lancet*, vol. 359, pp. 572–577, 2002.

[5] G. Ball et al., “An integrated approach utilizing artificial neural networks and SELDI mass spectrometry for the classification of human tumours and rapid identification of potential biomarkers,” *Bioinformatics*, vol. 18, pp. 395–404, 2002.

[6] W. Zhu et al., “Detection of cancer-specific markers amid massive mass spectral data,” in *Proc. Nat. Academy Sci. USA*, vol. 100, pp. 14666–14671, 2003.

[7] B. L. Adam et al., “Serum protein fingerprinting coupled with a pattern-matching algorithm distinguishes prostate cancer from benign prostate hyperplasia and healthy men,” *Cancer Res.*, vol. 62, pp. 3609–3614, 2002.

[8] A. Vlahou et al., “Diagnosis of ovarian cancer using decision tree classification of mass spectral data,” *J. Biomed. Biotechnol.*, vol. 2003, pp. 308–314, 2003.

[9] A. J. Rai et al., “Proteomic approaches to tumor marker discovery,” *Archives Pathol. Laboratory Med.*, vol. 126, pp. 1518–1526, 2002.

[10] Y. S. Qu et al., “Boosted decision tree analysis of surface-enhanced laser desorption/ionization mass spectral serum profiles discriminates prostate cancer from noncancer patients,” *Clinical Chemistry*, vol. 48, pp. 1835–1843, 2002.

[11] G. Izmirlian, “Application of the random forest classification algorithm to a SELDI-TOF proteomics study in the setting of a cancer prevention trial,” *Ann. NY Academy Sci.*, vol. 1020, pp. 154–174, 2004.

[12] B. L. Wu et al., “Comparison of statistical methods for classification of ovarian cancer using mass spectrometry data,” *Bioinformatics*, vol. 19, pp. 1636–1643, 2003.

[13] L. Li et al., “Data mining techniques for cancer detection using serum proteomic profiling,” *Artif. Intell. Med.*, vol. 32, pp. 71–83, 2004.

[14] J. S. Yu et al., “Ovarian cancer identification based on dimensionality reduction for high-throughput mass spectrometry data,” *Bioinformatics*, vol. 21, pp. 2200–2209, 2005.

[15] X. G. Zhang et al., “Recursive SVM feature selection and sample classification for mass-spectrometry and microarray data,” *BMC Bioinformat.*, vol. 7, article 197, 2006.

[16] Y. Yasui et al., “An automated peak identification/calibration procedure for high-dimensional protein measures from mass spectrometers,” *J. Biomed. Biotechnol.*, vol. 2003, pp. 242–248, 2003.

[17] R. Aebersold and M. Mann, “Mass spectrometry-based proteomics,” *Nature*, vol. 422, pp. 198–207, 2003.

[18] S. M. Hanash et al., “Mining the plasma proteome for cancer biomarkers,” *Nature*, vol. 452, pp. 571–579, 2008.

[19] R. Azencott, *Simulated Annealing: Parallelization Techniques*. New York, NY, USA: Wiley, 1992.

[20] S. Kirkpatrick et al., “Optimization by simulated annealing,” *Science*, vol. 220, pp. 671–680, 1983.

[21] E. Aarts and J. Korst, *Simulated Annealing and Boltzmann Machines*. New York, NY, USA: Wiley, 1989.

[22] A. Bouamrani et al., “Mesoporous silica chips for selective enrichment and stabilization of low molecular weight proteome,” *Proteomics*, vol. 10, pp. 496–505, 2010.

[23] A. Assareh and M. H. Moradi, “Extracting efficient fuzzy if-then rules from mass spectra of blood samples to early diagnosis of ovarian cancer,” in *Proc. IEEE Symp. Comput. Intell. Bioinformat. Comput. Biol.*, 2007, pp. 502–506.

[24] J. M. Sorace and M. Zhan, “A data review and re-assessment of ovarian cancer serum proteomic profiling,” *BMC Bioinformat.*, vol. 4, 2003. Q5

[25] G. Alexe et al., “Ovarian cancer detection by logical analysis of proteomic data,” *Proteomics*, vol. 4, pp. 766–783, 2004.

[26] J.-K. Yu et al., “An integrated approach to the detection of colorectal cancer utilizing proteomics and bioinformatics,” *World J. Gastroenterol*, vol. 10, pp. 3127–3131, 2004.

[27] Y. J. Engwegen et al., “Identification of serum proteins discriminating colorectal cancer patients and healthy controls using surface-enhanced laser desorption ionisation-time of flight mass spectrometry,” *World J. Gastroenterol*, vol. 12, pp. 1536–1544, 2006.

[28] D. F. Ransohoff et al., “Assessment of serum proteomics to detect large colon adenomas,” *Cancer Epidemiol Biomarkers Prev*, vol. 17, pp. 2188–2193, 2008.

Queries to the Author

Q1. Please check whether the affiliations for all the authors are ok as set.
Q2. Figure 1 is mismatch with provided pdf. We have followed source file. Please check.
Q3. Table 3 is not cited in the text. Please cite table 3 in the text at appropriate place/places.
Q4. Please provide names of all the author's in the references.
Q5. Please provide page range for reference [24].